

# ESTIMATING EFFECTIVE HYDRAULIC CONDUCTIVITY ( $K_e$ ) FOR THE RANGELAND HYDROLOGY AND EROSION MODEL (RHEM)



Osama Zuhair Al-hamdan<sup>1,\*</sup>, C. Jason Williams<sup>2</sup>, Fred B. Pierson<sup>3</sup>, Mariano Hernandez<sup>4</sup>, S. Kossi Nouwakpo<sup>5</sup>

<sup>1</sup> Department of Civil and Architectural Engineering, Texas A&M University, Kingsville, Texas, USA.

<sup>2</sup> Southwest Watershed Research Center, USDA ARS, Tucson, Arizona, USA.

<sup>3</sup> Northwest Watershed Research Center, USDA ARS, Boise, Idaho, USA.

<sup>4</sup> Natural Resources and the Environment, University of Arizona, Tucson, Arizona, USA.

<sup>5</sup> Northwest Irrigation and Soils Research Lab, USDA ARS, Kimberly, Idaho, USA.

\* Correspondence: osama.al-hamdan@tamuk.edu, osamaalhamdan@gmail.com

## HIGHLIGHTS

- Effective hydraulic conductivity ( $K_e$ ) predictive equations in all RHEM versions have satisfactory performance.
- New  $K_e$  predictive equations were developed for RHEM applications over broader rangeland conditions.
- $K_e$  values on most rangelands can be estimated through readily measurable ground cover and soil texture data.

**ABSTRACT.** *Effective hydraulic conductivity ( $K_e$ ) is an important parameter for the prediction of infiltration and runoff by the Rangeland Hydrology and Erosion Model (RHEM). Three sets of equations to predict  $K_e$  have previously been used in RHEM. These equations are mainly based on rainfall simulation data representing undisturbed sites and have not undergone comprehensive evaluation for various rangeland conditions, particularly after disturbances. The goal of this research was to evaluate these equations using independent data obtained from rainfall simulations conducted at multiple rangeland sites. Additionally, we developed and evaluated a new set of  $K_e$  predictive equations applying readily measurable cover and soils data spanning a wide range of vegetation, soil textures, and disturbance conditions. The results show that all previous  $K_e$  equations in RHEM have a “satisfactory” performance with index of agreement ( $d$ ) > 0.75 and  $R^2$  > 0.4. The new  $K_e$  approach resulted in “very good” performance with  $d$  > 0.9 and  $R^2$  > 0.5. The new set of equations enhances RHEM for applications over broader rangeland conditions, including sparse vegetation cover following disturbances or community transitions.*

**Keywords.** Disturbed Rangelands, Hillslope Runoff, Infiltration.

The Rangeland Hydrology and Erosion Model (RHEM) (Al-Hamdan et al., 2015; Hernandez et al., 2017) is an event-based model that estimates runoff, erosion, and sediment delivery rates and volumes at the spatial scale of the hillslope and the temporal scale of a single rainfall event. To effectively predict the erosion component, the model must first accurately predict the associated runoff. In RHEM, runoff is modeled as Hortonian overland flow, where it is assumed to exist only when the rainfall rate exceeds the infiltration rate (Horton, 1933). The infiltration component in RHEM is computed using a three-parameter infiltration equation (Parlange et al., 1982), in

which the models of Green and Ampt (1911) and Smith and Parlange (1978) are included as two limiting cases. In both cases, RHEM uses the effective hydraulic conductivity ( $K_e$ ) as the key parameter for modeling infiltration rate. The  $K_e$  parameterization approaches in RHEM utilize commonly available soil and vegetation data, such as vegetation cover and soil texture class (Al-Hamdan et al., 2015; Hernandez et al., 2017). The existing parameterization methods in RHEM were designed to estimate  $K_e$  for a fairly broad spectrum of soil textures, vegetation types, and undisturbed ground cover conditions. Nevertheless, there is a scarcity of studies that have thoroughly evaluated these approaches using field data across diverse rangeland conditions, particularly after disturbances. While RHEM includes a method to estimate the impact of salinity on  $K_e$ , it lacks specific parameterization approaches for predominantly bare or disturbed conditions, like those occurring immediately after a wildfire or with prolonged woody plant encroachment. The purpose of this study was to assess and enhance infiltration parameterization for the application of the RHEM tool over diverse rangeland conditions. The specific objectives of this research were to:

Submitted for review on 30 April 2023 as manuscript number NRES 15652; approved for publication as a Research Article by Associate Editor Dr. Prem Parajuli and Community Editor Dr. Kati Migliaccio of the Natural Resources & Environmental Systems Community of ASABE on 18 October 2023.

Mention of company or trade names is for description only and does not imply endorsement by the USDA. The USDA is an equal opportunity provider and employer.

- Evaluate three existing sets of equations, used in the RHEM model to predict  $K_e$ .
- Develop and evaluate an alternative set of  $K_e$  parameter estimation equations that uses readily measurable vegetation data for a wider range of vegetation, ground cover, and soil conditions.
- Establish a parameterization approach to estimate  $K_e$  for RHEM for diverse rangeland conditions.

## INFILTRATION MODEL DESCRIPTION

To compute the infiltration rate, RHEM applies an approach based on the kinematic runoff and erosion model (KINEROS2) (Smith et al., 1995), which utilizes a three-parameter infiltration equation (Parlange et al., 1982):

$$f = K_e \left[ 1 + \frac{\alpha}{\exp\left(\frac{\alpha I}{(G+h)(\theta_s - \theta_i)}\right) - 1} \right] \quad (1)$$

where

$f$  = the infiltration capacity ( $\text{m s}^{-1}$ )

$K_e$  = the soil effective saturated hydraulic conductivity ( $\text{m s}^{-1}$ )

$\alpha$  = a parameter between 0 and 1

$\exp$  = exponential function with base Euler's number ( $e$ )

$I$  = the cumulative depth of the water infiltrated into the soil (m)

$G$  = the integrated capillary head across the wetting front (m)

$h$  = the depth of surface flow (m)

$\theta_s$  = the soil porosity ( $\text{m}^3 \text{ m}^{-3}$ )

$\theta_i$  = the initial (antecedent) soil moisture content (Smith et al., 1993).

When  $\alpha = 0$ , equation 1 is reduced to the familiar Green and Ampt infiltration model (Green and Ampt, 1911), and when  $\alpha = 1$ , the equation simplifies to the Smith and Parlange model (Smith and Parlange, 1978). Poulovassilis and Argyrokastritis (2020) presented the values of parameter  $\alpha$  across various soil types, revealing a trend of increasing  $\alpha$  value as the soil becomes finer. However, they proposed to use a fixed  $\alpha$  value for practical purposes and thus convert the equation into a two-parameter equation. Demonstrations in Parlange et al. (1982), and other experimental and numerical results, indicate that a value of  $\alpha$  on the order of 0.8 to 0.85 is commonly a best fit for most natural soils (Smith et al., 1993; Hernandez et al., 2017). For RHEM, the default value of  $\alpha$  for the versions RHEM V2.2, RHEM V2.3, and RHEM V2.4 is 0.8, while earlier versions of the model have the default value of  $\alpha$  as 0.03.

To calculate infiltration rate for a given initial soil moisture, and fixed  $\alpha$  value, equation 1 requires the values of  $G$ , and  $K_e$ . RHEM applies values of  $G$  based on soil texture, consistent with KINEROS2 (Hernandez et al., 2017). Therefore,  $K_e$  is the parameter that is used to characterize sites for calculation of infiltration based on vegetation cover.

## K. PARAMETERIZATION APPROACHES IN RHEM

Based on two parameterization approaches, RHEM has previously used three sets of equations to calculate  $K_e$  ( $\text{mm hr}^{-1}$ ) which are utilized in RHEM V2.1, V2.3 and V2.4. As a first approach,  $K_e$  is calculated using equation 2 from Nearing et al. (2011), as applied in RHEM V2.1:

$$\ln K_e = 0.174 + 2.975V_g + 0.923V_f - 1.450cl \quad (2)$$

where

$V_g$  = the fraction of total ground cover underneath and outside of the vegetative canopy ( $\text{m}^2 \text{ m}^{-2}$ ) inclusive of rock and gravel >5 mm, litter in contact with the soil surface, plant basal area, and cryptogams

$V_f$  = the fraction of standing live and dead foliar cover ( $\text{m}^2 \text{ m}^{-2}$ )

$cl$  = the fraction of clay content of surface soil ( $\text{g}^1 \text{ g}^{-1}$ ).

In the second approach,  $K_e$  is calculated using baseline hydraulic conductivity ( $K_b$ ) adjusted exponentially based on plant basal cover and litter ground cover, as shown in equation 3:

$$K_e = K_b e^{c(basal+litter)} \quad (3)$$

where

$K_b$  = the baseline saturated hydraulic conductivity ( $\text{mm hr}^{-1}$ ) for a given soil texture class

$e$  = Euler's number

$c$  = adjustment coefficient for a given soil texture class

$basal$  = the plant basal area cover fraction ( $\text{m}^2 \text{ m}^{-2}$ )

$litter$  = litter cover fraction ( $\text{m}^2 \text{ m}^{-2}$ ).

In RHEM V2.3,  $K_e$  is estimated using a set of equations that are based on equation 3, in which  $K_b$  is the 25<sup>th</sup> percentile saturated hydraulic conductivity for each soil textural class, as reported by Rawls et al. (1998), and  $c$  is the natural log of the ratio of the geometric mean to the 25<sup>th</sup> percentile values of saturated hydraulic conductivity (Hernandez et al., 2017). RHEM V2.4 uses a modified set of equations in which certain  $K_b$  and  $c$  were obtained from Stone et al. (1992), who used and adjusted the values based on values reported by Rawls et al. (1982).

In both approaches (all three sets of equations), the  $K_e$  value is adjusted based on the associated vegetation community, with  $K_e$  multiplied by 0.8, 1.0, 1.0, and 1.2 when applying the equation for sod grass, bunch grass, forb, and shrub communities, respectively (Nearing et al., 2011; Hernandez et al., 2017).

## MATERIALS AND METHODS

To achieve the objectives of this study, three data sets from different rainfall simulation field experiments were used. Subsequent sections describe each data set.

### DATA USED FOR TESTING PREVIOUS APPROACHES AND DEVELOPING NEW $K_e$ EQUATIONS

Two data sets were used to evaluate the three sets of equations. The first set included rainfall simulation experiment data collected by the Water Erosion Prediction Project (WEPP) (Johnson and Blackburn, 1989; Simanton et al.,

1991; Laflen et al., 1991), the Interagency Rangeland Water Erosion Team (IRWET) (Franks et al., 1998), and the National Range Study Team (NRST) (Franks et al., 1998; Pierson et al., 2002) studies. In these studies, a rotating-boom rainfall simulator (Swanson, 1965) was used to simulate rainfall for 30 minutes at about 60 mm hr<sup>-1</sup> intensity. Each plot was pre-wet 24 hours earlier by conducting a rotating-boom rainfall simulation at the initial soil moisture for one hour at 60 mm hr<sup>-1</sup> intensity. The data include Natural (undisturbed) and Bare (standing vegetation was removed to the ground by clipping and ground cover was removed by hand) treatments (Johnson and Blackburn, 1989). The plots were 10.7 m long and 3.05 m wide, with the long borders oriented perpendicular to the hillslope contour. Ground cover, foliar cover, and foliar life form were measured for all plots using a point-frequency-frame. The vegetation community of each plot was decided based on the dominant

measured life form. The combined data sets cover a wide range of soil textures and vegetation types (table 1). Soil texture, ground surface slope, sediment rates, and runoff were measured for each plot. For the current study,  $K_e$  was optimized based on the total volume of runoff for each plot. By using optimized  $K_e$  values, average total runoff converged within less than a 0.02 mm of the average of the measured total runoff for all plots. Optimized  $K_e$  was used to develop the new  $K_e$  estimating equation.

## DATA USED FOR EVALUATING PREVIOUS APPROACHES AND NEW $K_e$ EQUATIONS

A third set of data was used to evaluate the previous and new parameterization approaches in RHEM. Those data were obtained from independent rainfall simulation experiments conducted by the United States Department of Agriculture-Agricultural Research Service (USDA-ARS)

**Table 1. Experimental sites used to test previous sets of equations and develop the new  $K_e$  parameterization approach.**

Site	Location	Soil Texture	No. of Plots	Treatments	Slope	Average Calibrated $K_e$ (mm h <sup>-1</sup> )
A187 <sup>[a]</sup>	Tombstone, Arizona	Sandy clay loam	4	Natural, Bare	0.1	12.4, 0.3
A287 <sup>[b]</sup>	Tombstone, Arizona	Sandy loam	1	Natural	0.04	7.6
C187 <sup>[c]</sup>	Sonora, Texas	Silty clay	3	Natural, Bare	0.083	4.4, 0.4
Coyote87 <sup>[a]</sup>	Coyote Butte, Idaho	Silt loam	4	Natural, Bare	0.101	19.6, 4.6
D187 <sup>[b]</sup>	Chickasha, Oklahoma	Sandy loam	3	Natural, Bare	0.05	4.6, 0.4
D287 <sup>[b]</sup>	Chickasha, Oklahoma	Sandy loam	4	Natural, Bare	0.05	5.5, 0.6
E287 <sup>[b]</sup>	Freedom, Oklahoma	Loam	3	Natural, Bare	0.06	16.8, 1.5
F187 <sup>[d]</sup>	Sidney, Montana	Loam	4	Natural, Bare	0.103	21, 4.6
G187 <sup>[a]</sup>	Meeker, Colorado	Silty clay	2	Bare	0.1	4.7
H187 <sup>[b]</sup>	Cottonwood, South Dakota	Clay	1	Bare	0.09	0.6
H287 <sup>[b]</sup>	Cottonwood, South Dakota	Clay	4	Natural, Bare	0.118	3.5, 0.4
I187 <sup>[d]</sup>	Los Alamos, New Mexico	Loam	4	Natural, Bare	0.068	7.2, 1.6
J187 <sup>[c]</sup>	Cuba, New Mexico	Sandy loam	4	Natural, Bare	0.07	14.3, 3.7
K187 <sup>[a]</sup>	Susanville, California	Loam	2	Natural	0.11	26.9
Nancy87 <sup>[a]</sup>	Reynolds, Idaho	Silt loam	4	Natural, Bare	0.059	10.5, 6.5
Summit87 <sup>[a]</sup>	Summit, Idaho	Sandy loam	4	Natural, Bare	0.09	16.0, 13.8
D188 <sup>[b]</sup>	Chickasha, Oklahoma	Sandy loam	4	Natural, Bare	0.05	16.1, 1.3
D288 <sup>[b]</sup>	Chickasha, Oklahoma	Sandy loam	4	Natural, Bare	0.048	10.8, 1.8
E288 <sup>[b]</sup>	Freedom, Oklahoma	Loam	4	Natural, Bare	0.06	27.2, 1.9
E588 <sup>[b]</sup>	Woodward, Oklahoma	Loam	3	Natural, Bare	0.06	18.6, 5.6
H188 <sup>[b]</sup>	Cottonwood, South Dakota	Clay	2	Natural	0.08	6.5
H288 <sup>[b]</sup>	Cottonwood, South Dakota	Clay	1	Natural	0.12	2.6
K188 <sup>[a]</sup>	Susanville, California	Loam	3	Natural, Bare	0.117	29.5, 6.6
B190 <sup>[c]</sup>	Wahoo, Nebraska	Clay loam	2	Natural	0.1	2.2
B290 <sup>[b]</sup>	Wahoo, Nebraska	Clay loam	5	Natural	0.11	12.1
C190 <sup>[b]</sup>	Amarillo, Texas	Clay loam	5	Natural	0.03	10.6
C290 <sup>[c]</sup>	Amarillo, Texas	Loam	3	Natural	0.02	10.0
E191 <sup>[d]</sup>	Eureka, Kansas	Silty clay	6	Natural	0.05	17.3
E291 <sup>[b]</sup>	Eureka, Kansas	Silty clay	2	Natural	0.05	16.9
E391 <sup>[c]</sup>	Eureka, Kansas	Silty clay	5	Natural	0.03	3.4
F191 <sup>[b]</sup>	Akron, Colorado	Sandy clay loam	5	Natural	0.074	4.6
F291 <sup>[b]</sup>	Akron, Colorado	Sandy loam	6	Natural	0.08	13.9
F391 <sup>[c]</sup>	Akron, Colorado	Sandy clay loam	5	Natural	0.066	5.0
G191 <sup>[b]</sup>	Newcastle, Wyoming	Sandy loam	6	Natural	0.06	28.1
G291 <sup>[b]</sup>	Newcastle, Wyoming	Sandy loam	5	Natural	0.084	29.7
G391 <sup>[b]</sup>	Newcastle, Wyoming	Sandy loam	5	Natural	0.074	11.4
H192 <sup>[b]</sup>	Killdeer, North Dakota	Sandy loam	4	Natural	0.123	42.5
H292 <sup>[b]</sup>	Killdeer, North Dakota	Sandy loam	6	Natural	0.113	20.2
H392 <sup>[b]</sup>	Killdeer, North Dakota	Sandy loam	6	Natural	0.01	16.9
I192 <sup>[a]</sup>	Buffalo, Idaho	Clay loam	6	Natural	0.011	9.7
I292 <sup>[b]</sup>	Buffalo, Idaho	Clay loam	4	Natural	0.068	10.7
J192 <sup>[a]</sup>	Blackfoot, Idaho	Silt loam	6	Natural	0.077	21.2
J292 <sup>[b]</sup>	Blackfoot, Idaho	Silt loam	5	Natural	0.08	19.5
K192 <sup>[b]</sup>	Prescott, Arizona	Loam	6	Natural	0.052	12.0
K292 <sup>[b]</sup>	Prescott, Arizona	Loam	6	Natural	0.05	10.5

[a] Predominantly Shrub.

[b] Predominantly Bunch Grass.

[c] Predominantly Sod Grass.

[d] Predominantly Forb.

Northwest Watershed Research Center, Boise, Idaho (Pierson et al., 2007, 2009, 2010, 2013; Moffet et al., 2007; Williams et al., 2014). These experiments applied a Colorado State University type rainfall simulator (Holland, 1969) consisting of multiple stationary sprinklers elevated 3.05 m above the ground surface (Pierson et al., 2007, 2009, 2010, 2013). Data were obtained for multiple sites, including sagebrush sites that have been encroached by conifers and/or burned by prescribed fire or wildfire. The plot length in this group varied from 6 m to 7 m and width varied from 2 m to 5 m, again with the longer borders oriented perpendicular to the hillslope contour. The rainfall intensity and duration varied among sites (table 2). Usually, plots were pre-wet by applying rainfall simulation for a specific period of time under dry antecedent soil moisture conditions.

## STATISTICAL ANALYSIS

Statistical analyses were conducted using SAS software, version 9.4 (SAS Institute Inc., 2015). Multiple stepwise linear regression analyses were used to derive the relationship between  $K_e$  as a dependent variable and ground and foliar cover attributes, slope, and soil texture as independent variables. The general linear model was used to test the significance of differences between  $K_e$  mean values among vegetation communities. Prior to this analysis, values of  $K_e$  were log transformed to address deviation from normality as well as to improve homoscedasticity and linearity (Allison, 1999).

Piecewise (segmented) regression analysis was applied, in which two continuous relationships between the log-transformed  $K_e$  and the independent variables were fitted to improve the linear relationship (Ryan et al., 2002, 2005). The PROC NLIN analysis technique in SAS was used to find the breakpoint at which the relationship between  $K_e$  and vegetation ground cover changed (Ryan and Porth, 2007).

A significance level of 0.05 was used for all statistical tests, including the criteria for including the variables in the multiple regressions. The coefficient of determination ( $R^2$ ; in conjunction with the gradient and intercept of the corresponding regression line) and the index of agreement ( $d$ ) (Willmott, 1981) were used to evaluate the applicability of the hydraulic conductivity equations in RHEM.  $R^2$  was calculated by:

$$R^2 = \left( \frac{\sum_{i=1}^n (O_i - O_{avg})(M_i - M_{avg})}{\sqrt{\sum_{i=1}^n (O_i - O_{avg})^2} \sqrt{\sum_{i=1}^n (M_i - M_{avg})^2}} \right)^2 \quad (4)$$

and  $d$  was calculated by:

$$d = 1 - \frac{\sum_{i=1}^n (O_i - M_i)^2}{\sum_{i=1}^n (|M_i - O_{avg}| + |O_i - O_{avg}|)} \quad (5)$$

where

$O_i$  = the ith observation to be evaluated

$M_i$  = the simulated value by the model for the corresponding ith observation

$O_{avg}$  = the average of the observed (measured) values

$M_{avg}$  = the average of the simulated values by the model

$n$  = the number of observations.

For a good agreement,  $R^2$  should be close to one, the corresponding intercept should be close to zero and the gradient should be close to one. Performance of the runoff prediction at the monthly temporal scales is considered “Very Good” when  $d > 0.90$ , “Good” when  $0.85 < d \leq 0.90$ , “Satisfactory” when  $0.75 < d \leq 0.85$ , and “Unsatisfactory” when  $d \leq 0.75$  (Moriasi et al., 2015). Given that event-based predictions are usually less accurate than monthly ones, using these performance levels for this study is considered a more rigorous performance evaluation.

## RESULTS AND DISCUSSION

### RANGES OF VARIABLES VALUES

For  $\alpha$  as 0.8, optimized  $K_e$  values that were used to develop the new equations varied from near zero to 38.6 mm hr<sup>-1</sup>. Measured total runoff values varied from 0.1 to 31.2 mm. Clay texture fraction varied from 0.06 to 0.51. Silt texture fraction varied from 0.16 to 0.68. Vegetation ground cover (basal, litter, and cryptograms) varied from 0 to 1.0, while foliar cover varied from 0 to 0.91. The data used to develop and evaluate the equations represent a wide array of ground cover and soil texture variations. The ground cover data represents all possible values to find on rangelands, while  $K_e$  values cover measured geometric mean measurements for most soil texture types in Rawls' et al. (1998) data, with the exceptions of sandy and sandy loam.

### $K_e$ ESTIMATION EQUATIONS

A multiple regression equation between the logarithm of  $K_e$  as a dependent variable and vegetation ground cover (litter cover and plant basal cover) ( $V_G$ ), vegetation foliar cover, clay ( $Cl$ ), and silt ( $Si$ ) amounts as independent variables resulted in the following equation:

$$\ln K_e = 0.9717 + 1.81*V_G + 1.059*V_F - 3.1325*Cl \quad (n = 180, R^2 = 0.52) \quad (6)$$

Table 2. Experimental sites used to evaluate the  $K_e$  parameterization approaches.

Site	Location	Soil Texture	No. of Plots	Treatment or Disturbance	Slope	Average Calibrated $K_e$ (mm hr <sup>-1</sup> )
Breaks	Reynolds Creek, Idaho	Sandy loam	28	Natural, fire	0.426	32, 32.7
Castlehead	Owyhee County, Idaho	Stoney loam	18	Tree encroachment, wildfire	0.172	24.5, 17.6
Marking Corral	White Pine County, Nevada	Gravelly loam	22	Tree encroachment, fire	0.097	22.2, 37.1
Onaqui	Tooele County, Utah	Gravelly loam	29	Tree encroachment, fire	0.16	30.3, 24.8
Steens	Harney County, Oregon	Gravelly silt loam	10	Tree encroachment, ten years after tree cut	0.186	31.3, 22.7

Applying the segmented regression analysis using the same variables of equation 6 resulted in the following equation:

$$\ln K_e = \begin{cases} 0.7211 + 3.0911 * V_G \\ \quad + 1.1052 * V_F - 3.8344 * Cl & \text{if } V_G \leq 0.7143 \\ 4.4624 - 2.2377 * V_G \\ \quad + 1.1052 * V_F - 3.8344 * Cl & \text{if } V_G > 0.7143 \end{cases} \quad (7)$$

Applying the general linear regression analysis, where plant life form is the categorical variable, along with the piecewise approach, resulted in the following equations:

Bunch Grass:

$$\ln K_e = \begin{cases} 0.1638 + 4.6152 * V_G \\ \quad + 0.6098 * V_F - 2.9387 * Cl & \text{if } V_G \leq 0.5071 \\ 2.3925 + 0.2202 * V_G \\ \quad + 0.6098 * V_F - 2.9387 * Cl & \text{if } V_G > 0.5071 \end{cases} \quad (8)$$

Sod Grass:

$$\ln K_e = \begin{cases} -0.426 + 4.6152 * V_G \\ \quad + 0.6098 * V_F - 2.9387 * Cl & \text{if } V_G \leq 0.5071 \\ 1.8027 + 0.2202 * V_G \\ \quad + 0.6098 * V_F - 2.9387 * Cl & \text{if } V_G > 0.5071 \end{cases} \quad (9)$$

Shrub:

$$\ln K_e = \begin{cases} 0.6788 + 4.6152 * V_G \\ \quad + 0.6098 * V_F - 2.9387 * Cl & \text{if } V_G \leq 0.5071 \\ 2.9075 + 0.2202 * V_G \\ \quad + 0.6098 * V_F - 2.9387 * Cl & \text{if } V_G > 0.5071 \end{cases} \quad (10)$$

Forb:

$$\ln K_e = \begin{cases} 0.6862 + 4.6152 * V_G \\ \quad + 0.6098 * V_F - 2.9387 * Cl & \text{if } V_G \leq 0.5071 \\ 2.9149 + 0.2202 * V_G \\ \quad + 0.6098 * V_F - 2.9387 * Cl & \text{if } V_G > 0.5071 \end{cases} \quad (11)$$

Equation 6 shows that  $K_e$  is significantly dependent on vegetation cover and clay ( $p < 0.05$ ). The equation is similar to the one applied in RHEM V2.1 in terms of independent parameters since some of the plots used to develop new equations were also used in developing equation 2. However, the new equations were developed using an expanded dataset (bare treatment). The coefficient of determination in the single segmented regression analysis ( $R^2 = 0.59$ ) was greater than in the analysis resulting in equation 6 ( $R^2 = 0.52$ ). Applying the general linear model and segmented

regression by dominant vegetation life form (shrub, forb, bunch grass, and sod grass) improved  $R^2$ , with a slight increase ( $R^2 = 0.64$ ) compared to equation 7.

Figure 1 shows an example of values obtained from equations 7 through 11 as a function of vegetation ground cover. The breakpoints generated by the piecewise regression in equations 7 through 11 identify a threshold at which there is a change in the infiltration rate with respect to vegetation ground cover. Using equation 7 for simplicity instead of equations 8 through 11 will not change prediction performance significantly, given the slight difference in  $R^2$  values between the two methods. However, the variable coefficients (sensitivity to variables) and the breakpoints are different. The differences are driven by (1) a relatively large concentration of shrub plots with low cover and high  $K_e$  and (2) a large number of sod grass plots with high cover and low  $K_e$ . Hence, when applying the segmented regression for all data points combined (eq. 7), the best-fit segmented line reflects these different diverging ends. These trends indicate the application of community-specific  $K_e$  equations may be useful when comparing hydrologic responses for respective ecological sites. Even though equations 8 through 11 have small differences in coefficients, the application of community-specific  $K_e$  equations could still lead to a high percentage of difference between two sites with low infiltration values because they are logarithmic relationships. The  $K_e$  values were greatest for shrub and forb cover types, slightly less, respectively, for the bunch grass cover type, and lowest for the sod grass cover type (fig. 1). These trends in  $K_e$  by cover type were consistent with those reported by Nearing et al. (2011) for RHEM V2.1. In the current study,  $K_e$  increased with vegetation ground cover before reaching a near steady state and subsequently declining slightly for the highest cover conditions (fig. 1). The slight decline at high cover values was potentially due to cover effects at the ground surface and/or alteration of rock cover effects on infiltration. Substantial live and senesced vegetation lying horizontally across the ground surface can shed rainfall and facilitate runoff (Pierson et al., 2008; Williams et al., 2016). Similarly, ample vegetation and ground cover can alter the effects of underlying rock cover on infiltration and runoff. The literature on rock cover effects on infiltration is contradictory

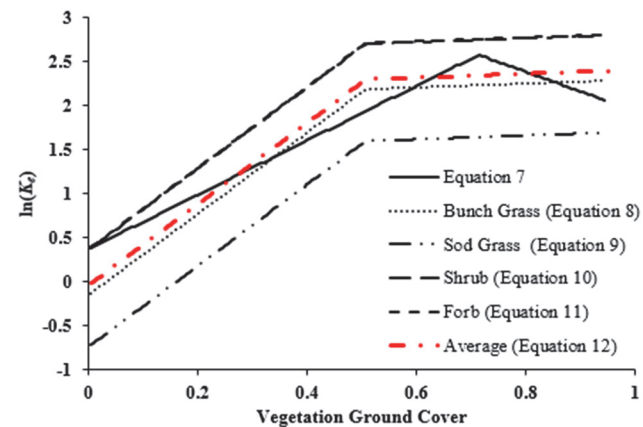


Figure 1. Values of  $\ln(K_e)$  using equations 7, 8 (Bunch Grass), 9 (Sod Grass), 10 (Shrub), 11 (Forb), and equation 12 versus vegetation ground cover when foliar cover is 0.1 and soil clay fraction is 0.1.

(Kidwell et al., 1997), depending on whether the rock cover is under a plant canopy or in the interspace area between plant canopies. Rock cover has been shown to enhance infiltration when resting on the soil surface and to impede infiltration where embedded in the soil surface (Poesen et al., 1990). Regardless, an increase in vegetation ground cover closer to 100% would replace the cover impact of rock. In the case where dominant plant life forms are known, equations 8 through 11 can be used. If the dominant plant life form is unknown or hard to define, then one can apply equation 7. However, for consistency, the following equation that gives an average  $K_e$  value based on the average value of coefficients from equations 8-11 can be used:

$$\ln K_e = \begin{cases} 0.2757 + 4.6152 * V_G \\ \quad + 0.6098 * V_F - 2.9387 * Cl & \text{if } V_G \leq 0.5071 \\ 2.5044 + 0.2202 * V_G \\ \quad + 0.6098 * V_F - 2.9387 * Cl & \text{if } V_G > 0.5071 \end{cases} \quad (12)$$

#### **$K_e$ EQUATIONS EVALUATION:**

Figure 2 shows the measured  $\ln(K_e)$  values for each plot from the table 1 data set versus the estimated  $\ln(K_e)$  using all sets of equations. Like typical regression results, small values were overestimated, and large values were underestimated in most cases. However, the respective error was reduced the most when using the group-segmented equations (fig. 2f). The segmented approach and RHEM V2.1 equations showed the largest  $R^2$ . In addition, the segmented approach was more comprehensive since it was an equation with continuous clay values and not a look-up table based on soil texture. If each soil texture class is assigned a given clay value, then equations 6 or 7 could be used to develop a set of equations similar to the one used in RHEM V2.4. In this case, each soil texture class has a  $K_e$  estimation equation as a function of vegetation cover. For instance, applying equation 6 to selected soil textures results in the following equations:

$$\text{Clay Loam: } K_e = 0.9 * \exp(1.81 * V_G + 1.059 * V_F) \quad (13)$$

$$\text{Silt Loam: } K_e = 1.7 * \exp(1.81 * V_G + 1.059 * V_F) \quad (14)$$

$$\text{Sandy Loam: } K_e = 1.9 * \exp(1.81 * V_G + 1.059 * V_F) \quad (15)$$

$$\text{Loam: } K_e = 1.4 * \exp(1.81 * V_G + 1.059 * V_F) \quad (16)$$

$$\text{Sand: } K_e = 2.4 * \exp(1.81 * V_G + 1.059 * V_F) \quad (17)$$

The corresponding equations for equations 13 through 17 from RHEM V2.4 are:

$$\text{Clay Loam: } K_e = 0.5 * \exp(2.3026 * V_G) \quad (18)$$

$$\text{Silt Loam: } K_e = 1.2 * \exp(2.0149 * V_G) \quad (19)$$

$$\text{Sandy Loam: } K_e = 5 * \exp(1.1632 * V_G) \quad (20)$$

$$\text{Loam: } K_e = 2.5 * \exp(1.5686 * V_G) \quad (21)$$

$$\text{Sand: } K_e = 64 * \exp(0.3564 * V_G) \quad (22)$$

Similar to RHEM V2.1, equations 13 through 17 include vegetation ground cover and foliar cover as factors, whereas RHEM V2.4 only applies vegetation ground cover as a factor. However, the  $K_e$  values derived from both sets of equations are within similar ranges, except for those for sandy soils. None of the sites in table 1 have sandy soils. This suggests caution in applying the equations to sites with soil textures outside of the range in which the equations were developed. Excluding the sandy sites, the new equations still span a reasonably wide range of soil textures typical of rangelands.

#### **RHEM APPLICATION EVALUATION**

The performance of RHEM in predicting runoff when using the different sets of  $K_e$  equations was evaluated using the independent data of plots with rainfall simulations (table 2). When using the newly developed equations, the values of  $K_e$  were multiplied by 1.3 to account for the bias in the log transformation (Duan, 1983). Results show that all previous methods have “satisfactory” performance with  $d$  values greater than 0.75 (figs. 3a-c). These results agree with Williams et al. (2022), who reported that RHEM V2.3 effectively predicted runoff and erosion from 36 patch-scale rainfall simulation plots at two sagebrush rangelands. However, like Williams et al. (2022), in many plots with minimal actual runoff, the runoff was overestimated at these sites. The new approach has “very good” results with a  $d$  value greater than 0.9 (figs. 3d-e). In all regressions, the slope between predicted and measured runoff was below one, while the intercept was large, indicating that the simulations were overestimating small values. This error is reduced when applying the new approach, where the slope is closer to one and the intercept is closer to zero. However, in some plots with minimal actual runoff, the runoff was still overestimated (fig. 3d). Further examination of the data shows that many of these plots are in burned canopy areas. This indicates that the equations’ trend, at which removing vegetation cover decreases  $K_e$  and infiltration, which increases runoff, did not hold. This means that other potential factors should be investigated in future work. One possible explanation is the effect of ash cover. Ash can increase surface retention/storage and storage, consequently increasing the  $K_e$  value (Ebel, 2012). Another source of error could be the assumed default value of initial saturation (0.25) for some plots, especially those that were not pre-wetted. If initial saturation was set to a different value (0.1) for those dry antecedent simulations, results could be improved, where the slope is closer to one and the intercept is closer to zero (fig. 3e). The saturation value is perhaps less important for predicting average annual responses but is likely important for predicting responses in single-event simulations.

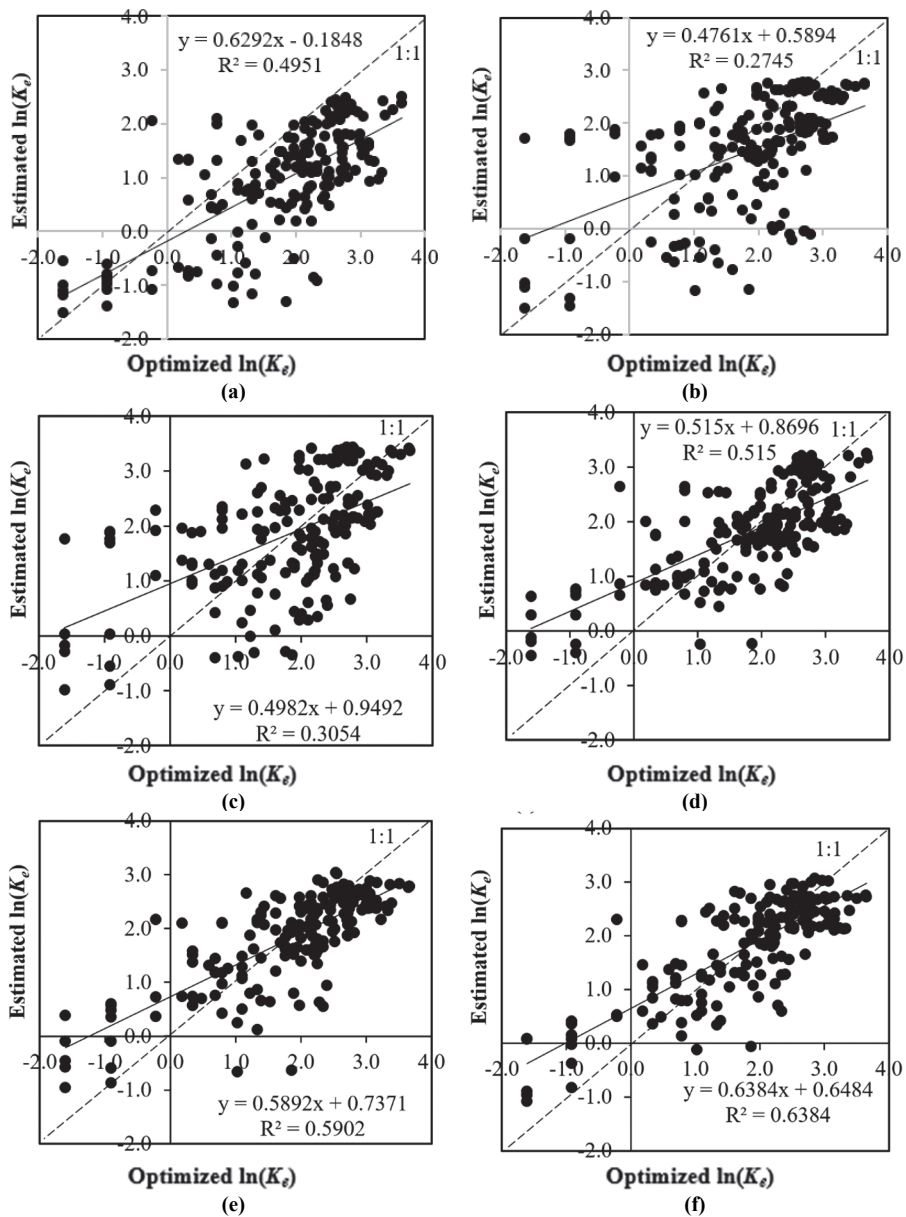


**Figure 2.** Measured  $\ln(K_e)$  values versus the estimated  $\ln(K_e)$  using (a) RHEM V2.1 equations, (b) RHEM V2.2 equations, (c) RHEM V2.4 equations, (d) equation 6, (e) equation 7, and (f) equations 8 through 11.

## SUMMARY AND CONCLUSION

In this study, three previously developed RHEM sets of equations for estimating  $K_e$  were evaluated with no calibration and showed “satisfactory” performance in estimating runoff with independent data. A new approach was also developed and tested using the same independent data. The new approach showed a “very good” performance in estimating runoff for RHEM at the plot scale. The new approach expands the applicability of RHEM for degraded or disturbed rangeland conditions with minimum vegetation cover. However, the new equations could be improved to address immediate post-fire conditions and soil textures outside the scope of the dataset applied in the current  $K_e$  parameterization approaches, such as for sands and loamy sands.

## ACKNOWLEDGMENTS

This study was conducted as a collaborative effort between the USDA Agricultural Research Service and Texas A&M University-Kingsville. Funding was provided by the USDA Agricultural Research Service. This article is Contribution No. 154 of the Sagebrush Steppe Treatment Evaluation Project (SageSTEP, [www.sagestep.org](http://www.sagestep.org)), funded by the U.S. Joint Fire Science Program, the Bureau of Land Management, and the National Interagency Fire Center.

## REFERENCES

- Al-Hamdan, O. Z., Hernandez, M., Pierson, F. B., Nearing, M. A., Williams, C. J., Stone, J. J.,... Weltz, M. A. (2015). Rangeland hydrology and erosion model (RHEM) enhancements for applications on disturbed rangelands. *Hydrol. Process.*, 29(3), 445-457. <https://doi.org/10.1002/hyp.10167>

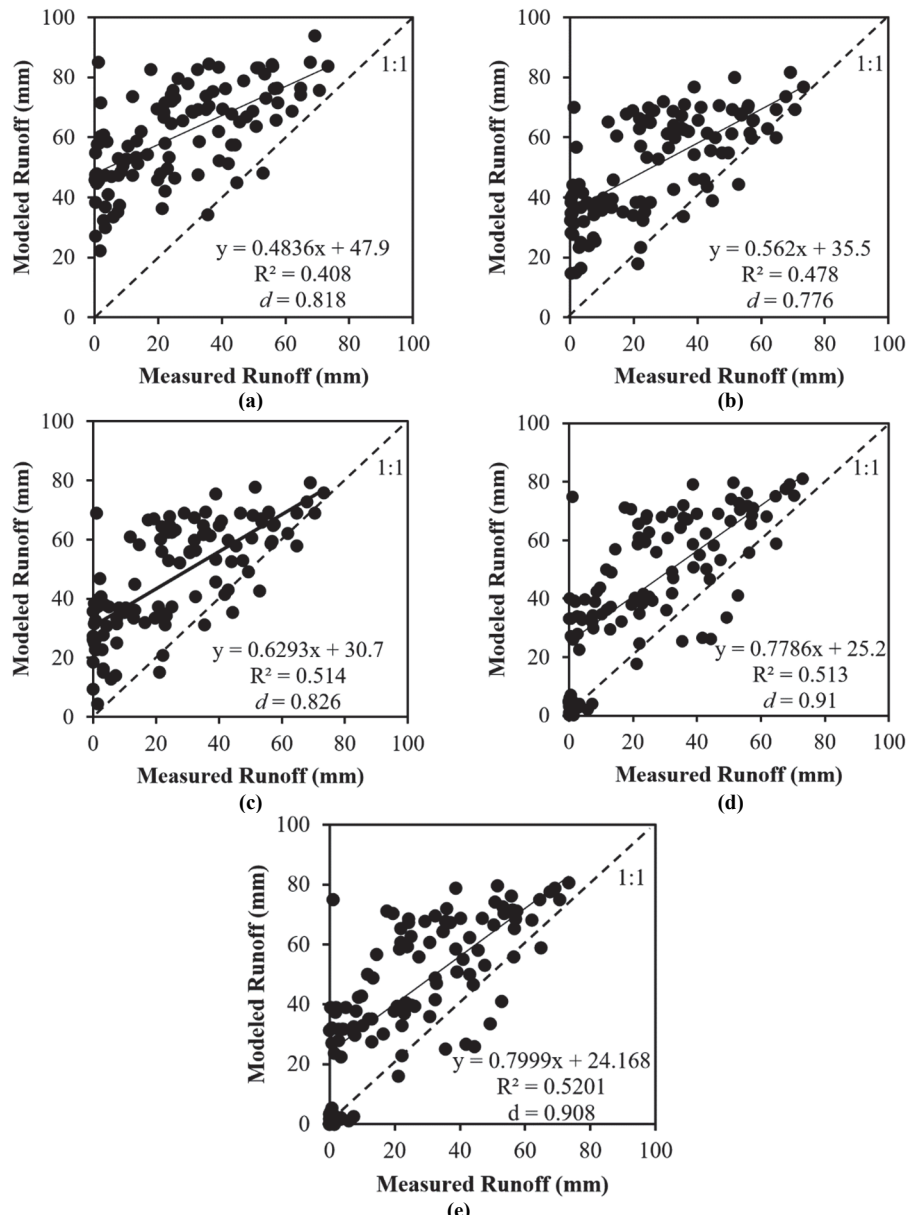


**Figure 3.** Measured runoff versus runoff estimated by RHEM when (a) using equations of RHEM V2.1 to estimate  $K_e$ , (b) using equations of RHEM V2.2 to estimate  $K_e$ , (c) using equations of RHEM V2.4 to estimate  $K_e$ , (d) using the new approach (eqs. 8 through 11) to estimate  $K_e$ , and (e) using the new approach (eqs. 8 through 11) to estimate  $K_e$  while setting initial saturation value as 0.1 for dry runs.

- Allison, P. D. (1999). *Multiple regression: A primer*. Oaks, CA: Pine Forge Press.
- Duan, N. (1983). Smearing estimate: A nonparametric retransformation method. *J. Am. Stat. Assoc.*, 78(383), 605-610. <https://doi.org/10.1080/01621459.1983.10478017>
- Ebel, B. A. (2012). Wildfire impacts on soil-water retention in the Colorado Front Range, United States. *Water Resour. Res.*, 48(12). <https://doi.org/10.1029/2012WR012362>
- Franks, C. D., Pierson, F. B., Mendenhall, A. G., Spaeth, K. E., & Weltz, M. A. (1998). Interagency rangeland water erosion project report and state data summaries. Interagency rangeland water erosion team (IRWET) and National Range Study Team (NRST). NWRC 98-1. Boise, ID: USDA-ARS, NRCS, Northwest Watershed Research Center.
- Green, W. H., & Ampt, A. G. (1911). Studies of soil physics. Part I - The flow of air and water through soils. *J. Agric. Sci.*, 4, 1-24. <https://doi.org/10.1017/S0021859600001441>

- Hernandez, M., Nearing, M. A., Al-Hamdan, O. Z., Pierson, F. B., Armendariz, G., Weltz, M. A.,... Collins, C. D. (2017). The rangeland hydrology and erosion model: A dynamic approach for predicting soil loss on rangelands. *Water Resour. Res.*, 53(11), 9368-9391. <https://doi.org/10.1002/2017WR020651>
- Holland, M. E. (1969). Design and testing of rainfall systems. CER 69-70 MEH 21. Fort Collins, CO: Colorado State University, Experimental Rainfall-Runoff Facility. Retrieved from <http://hdl.handle.net/10217/181126>
- Horton, R. E. (1933). The role of infiltration in the hydrologic cycle. *Eos Trans. AGU*, 14(1), 446-460. <https://doi.org/10.1029/TR014i001p00446>
- Johnson, C. W., & Blackburn, W. H. (1989). Factors contributing to sagebrush rangeland soil loss. *Trans. ASAE*, 32(1), 155. <https://doi.org/10.13031/2013.30975>
- Kidwell, M. R., Weltz, M. A., & Guertin, D. P. (1997). Estimation of green-ampt effective hydraulic conductivity for rangelands. *J. Range Manag.*, 50(3), 290-299. <https://doi.org/10.2307/4003732>

- Laflen, J. M., Elliot, W. J., Simanton, J. R., Holzhey, C. S., & Kohl, K. D. (1991). WEPP: Soil erodibility experiments for rangeland and cropland soils. *J. Soil Water Conserv.*, 46(1), 39-44.
- Moffet, C. A., Pierson, F. B., Robichaud, P. R., Spaeth, K. E., & Hardegree, S. P. (2007). Modeling soil erosion on steep sagebrush rangeland before and after prescribed fire. *CATENA*, 71(2), 218-228. <https://doi.org/10.1016/j.catena.2007.03.008>
- Moriasi, D. N., Gitau, M. W., Pai, N., & Daggupati, P. (2015). Hydrologic and water quality models: Performance measures and evaluation criteria. *Trans. ASABE*, 58(6), 1763-1785. <https://doi.org/10.13031/trans.58.10715>
- Nearing, M. A., Wei, H., Stone, J. J., Pierson, F. B., Spaeth, K. E., Weltz, M. A.,... Hernandez, M. (2011). A rangeland hydrology and erosion model. *Trans. ASABE*, 54(3), 901-908. <https://doi.org/10.13031/2013.37115>
- Parlange, J. Y., Lisle, I., Braddock, R. D., & Smith, R. E. (1982). The three-parameter infiltration equation. *Soil Sci.*, 133(6), 337-341. <https://doi.org/10.1097/00010694-198206000-00001>
- Pierson, F. B., Bates, J. D., Svejcar, T. J., & Hardegree, S. P. (2007). Runoff and erosion after cutting western juniper. *Rangel. Ecol. Manag.*, 60(3), 285-292. [https://doi.org/10.2111/1551-5028\(2007\)60\[285:RAEACW\]2.0.CO;2](https://doi.org/10.2111/1551-5028(2007)60[285:RAEACW]2.0.CO;2)
- Pierson, F. B., Moffet, C. A., Williams, C. J., Hardegree, S. P., & Clark, P. E. (2009). Prescribed-fire effects on rill and interrill runoff and erosion in a mountainous sagebrush landscape. *Earth Surf. Process. Landforms*, 34(2), 193-203. <https://doi.org/10.1002/esp.1703>
- Pierson, F. B., Robichaud, P. R., Moffet, C. A., Spaeth, K. E., Hardegree, S. P., Clark, P. E., & Williams, C. J. (2008). Fire effects on rangeland hydrology and erosion in a steep sagebrush-dominated landscape. *Hydrol. Process.*, 22(16), 2916-2929. <https://doi.org/10.1002/hyp.6904>
- Pierson, F. B., Spaeth, K. E., Weltz, M. A., & Carlson, D. H. (2002). Hydrologic response of diverse western rangelands. *J. Range Manag.*, 55(6), 558-570. <https://doi.org/10.2307/4003999>
- Pierson, F. B., Williams, C. J., Hardegree, S. P., Clark, P. E., Kormos, P. R., & Al-Hamdan, O. Z. (2013). Hydrologic and erosion responses of sagebrush steppe following juniper encroachment, wildfire, and tree cutting. *Rangeland Ecol. Manag.*, 66(3), 274-289. <https://doi.org/10.2111/REM-D-12-00104.1>
- Pierson, F. B., Williams, C. J., Kormos, P. R., Hardegree, S. P., Clark, P. E., & Rau, B. M. (2010). Hydrologic vulnerability of sagebrush steppe following pinyon and juniper encroachment. *Rangeland Ecol. Manag.*, 63(6), 614-629. <https://doi.org/10.2111/REM-D-09-00148.1>
- Poesen, J., Ingelmo-Sanchez, F., & Mucher, H. (1990). The hydrological response of soil surfaces to rainfall as affected by cover and position of rock fragments in the top layer. *Earth Surf. Process. Landforms*, 15(7), 653-671. <https://doi.org/10.1002/esp.3290150707>
- Poulouvassilis, A. & Argyrokastritis, I. (2020). A new approach for studying vertical infiltration. *Soil Res.* 58, 509-518.
- Rawls, W. J., Brakensiek, D. L., & Saxton, K. E. (1982). Estimation of soil water properties. *Trans. ASAE*, 25(5), 1316-1320. <https://doi.org/10.13031/2013.33720>
- Rawls, W. J., Gimenez, D., & Grossman, R. (1998). Use of soil texture, bulk density, and slope of the water retention curve to predict saturated hydraulic conductivity. *Trans. ASAE*, 41(4), 983-988. <https://doi.org/10.13031/2013.17270>
- Ryan, S. E., & Porth, L. S. (2007). A tutorial on the piecewise regression approach applied to bedload transport data. Gen. Tech. Rep. RMRS-GTR-189. Fort Collins, CO: USDA Forest Service, Rocky Mountain Research Station. <https://doi.org/10.2737/rmrs-gtr-189>
- Ryan, S. E., Porth, L. S., & Troendle, C. A. (2002). Defining phases of bedload transport using piecewise regression. *Earth Surf. Process. Landforms*, 27(9), 971-990. <https://doi.org/10.1002/esp.387>
- Ryan, S. E., Porth, L. S., & Troendle, C. A. (2005). Coarse sediment transport in mountain streams in Colorado and Wyoming, USA. *Earth Surf. Process. Landforms*, 30(3), 269-288. <https://doi.org/10.1002/esp.1128>
- SAS Institute Inc. (2015). Software Version 14.1. Cary, NC: SAS Institute Inc.
- Simanton, J. R., Weltz, M. A., & Larsen, H. D. (1991). Rangeland experiments to parameterize the water erosion prediction project model: Vegetation canopy cover effects. *J. Range Manag.*, 44(3), 276-282. <https://doi.org/10.2307/4002957>
- Smith, R. E., & Parlange, J.-Y. (1978). A parameter-efficient hydrologic infiltration model. *Water Resour. Res.*, 14(3), 533-538. <https://doi.org/10.1029/WR014i003p00533>
- Smith, R. E., Corradini, C., & Melone, F. (1993). Modeling infiltration for multistorm runoff events. *Water Resour. Res.*, 29(1), 133-144. <https://doi.org/10.1029/92WR02093>
- Smith, R. E., Goodrich, D. C., Woolhiser, D. A., & Unkrich, C. L. (1995). KINEROS - A kinematic runoff and erosion model. In V. P. Singh (Ed.), *Computer models of watershed hydrology* (pp. 697-732). Highlands Ranch, CO: Water Resources Publ.
- Stone, J. J., Lane, L. J., & Shirley, E. D. (1992). Infiltration and runoff simulation on a plane. *Transactions of the ASAE*, 35(1), 161-170. doi: 10.13031/2013.28583
- Swanson, N. P. (1965). Rotating-boom rainfall simulator. *Trans. ASAE*, 8(1), 71-72. <https://doi.org/10.13031/2013.40430>
- Williams, C. J., Pierson, F. B., Al-Hamdan, O. Z., Kormos, P. R., Hardegree, S. P., & Clark, P. E. (2014). Can wildfire serve as an ecohydrologic threshold-reversal mechanism on juniper-encroached shrublands. *Ecohydrology*, 7(2), 453-477. <https://doi.org/10.1002/eco.1364>
- Williams, C. J., Pierson, F. B., Al-Hamdan, O. Z., Nouwakpo, S. K., Johnson, J. C., Polyakov, V. O.,... Spaeth, K. E. (2022). Assessing runoff and erosion on woodland-encroached sagebrush steppe using the Rangeland Hydrology and Erosion Model. *Ecosphere*, 13(6), e4145. <https://doi.org/10.1002/ecs2.4145>
- Williams, C. J., Pierson, F. B., Kormos, P. R., Al-Hamdan, O. Z., Hardegree, S. P., & Clark, P. E. (2016). Ecohydrologic response and recovery of a semi-arid shrubland over a five year period following burning. *CATENA*, 144, 163-176. <https://doi.org/10.1016/j.catena.2016.05.006>
- Willmott, C. J. (1981). On the validation of models. *Phys. Geogr.*, 2(2), 184-194. <https://doi.org/10.1080/02723646.1981.10642213>